# Electrified distillation with flash vapor circulation and thermal storage for dynamic electricity markets

Qi, Meng; Zhang, Xiaodong; Wong, David Shan Hill; Shu, Chi Min; Cui, Chengtian; Kiss, Anton A.

**DOI**
10.1002/aic.18750

**Publication date**
2025

**Document Version**
Final published version

**Published in**
AIChE Journal

Received: 4 November 2024 | Revised: 26 December 2024 | Accepted: 20 January 2025

DOI: 10.1002/aic.18750

AIChE JOURNAL

RESEARCH ARTICLE

Process Systems Engineering

# Electrified distillation with flash vapor circulation and thermal storage for dynamic electricity markets

Meng Qi[1] | Xiaodong Zhang[2] | David Shan-Hill Wong[3] | Chi-Min Shu[4] | Chengtian Cui[5] | Anton A. Kiss[5]

[1]College of Chemistry and Chemical Engineering, China University of Petroleum (East China), Qingdao, China

[2]College of Smart Energy, Shanghai Jiao Tong University, Shanghai, China

[3]Department of Chemical Engineering, National Tsing Hua University, Hsinchu, Taiwan

[4]Department of Safety, Health, and Environmental Engineering, National Yunlin University of Science and Technology, Yunlin, Taiwan

[5]Department of Chemical Engineering, Delft University of Technology, Delft, The Netherlands

**Correspondence**
Chengtian Cui and Anton A. Kiss, Department of Chemical Engineering, Delft University of Technology, Van der Maasweg 9, 2629 HZ, Delft, The Netherlands.
Email: c.cui-1@tudelft.nl and a.a.kiss@tudelft.nl

**Funding information**
National Natural Science Foundation of China, Grant/Award Numbers: 22408402, 22208164; Shandong Provincial Postdoctoral Science Foundation, Grant/Award Number: SDBX2023020; Natural Science Foundation of Jiangsu Province, Grant/Award Number: BK20220348

## Abstract

Distillation is widely used for separating liquid mixtures, but its high heating demand poses challenges for achieving net-zero emissions. This study presents an innovative approach to electrifying distillation for load adaptability and flexible operation, aligning with dynamic electricity markets driven by renewables. The approach integrates flash vapor circulation and thermal storage into the distillation to optimize power usage and capitalizes on economic opportunities from load-flexible operation in response to fluctuating electricity pricing. A methanol/water distillation case study, using two typical electricity pricing scenarios, demonstrates that the proposed approach is more economically efficient than mechanical vapor recompression distillation, especially in lowering operational costs when the latter operates under fixed electricity pricing. However, compressor capital costs significantly impact overall costs, with sensitivity analysis examining different cost models. This approach can be applied to general distillation, allowing integration with the power sector and demand response programs, while enhancing flexibility, decarbonization, and efficiency.

**KEYWORDS**
decarbonization, design and scheduling optimization, distillation, flash vapor circulation, flexible operation, thermal storage

## 1 | INTRODUCTION

The rapid expansion of solar and wind power generation represents a major advancement in the integration of renewable energy into power grids. This shift is essential to the broader objective of decarbonizing the chemical industry, which relies on renewable electricity to meet the various energy needs of chemical processes.[1] A key initial step in this transition is the electrification of chemical processes, focusing on substituting conventional fossil fuel-based energy sources with renewable electricity.[2]

Distillation is a major energy consumer in the chemical industry, accounting for 60% of the energy used in all separation technologies.[3] However, its thermal efficiency is still leaving much to be desired.[4] Numerous approaches have been proposed to enhance efficiency and achieve decarbonization, such as adopting advanced distillation technologies and incorporating renewable energy sources for process

heating.[5–7] Among these, electrifying distillation and integrating it with renewable power supplies offers a promising solution.[8] Mature electrification technologies, including electric heaters (e-heaters), electrode boilers (e-boilers), and heat pumps, are widely utilized in distillation operations, each with distinct advantages and limitations. E-heaters and e-boilers offer nearly 100% power-to-heat efficiency, corresponding to a coefficient of performance (COP) of 1. E-heaters are versatile, operating across a broad temperature range of 200–1800°C,[9] while e-boilers effectively generate steam at 100–350°C,[5] covering most distillation process requirements. However, both are limited by their maximum COP of 1, offering no energy efficiency improvements beyond power input, with e-heaters potentially incurring higher operational costs at elevated temperatures. In contrast, heat pump-assisted distillation (HPAD),[10–12] such as the mechanical vapor recompression (MVR), vapor compression (VC), compression-resorption heat pump (CRHP), thermo-acoustic heat pump (TAHP), heat integrated distillation column (HIDiC), and so forth, provides significant primary energy savings of 20%–50% under certain conditions.[13] Among them, MVR is widely used in industrial applications, achieving a COP of up to 10 and making it a preferred option for process electrification. Despite its high efficiency, MVR requires a lower temperature lift to maintain its superior COP, limiting its applicability in processes needing substantial temperature differences. This balance of advantages and constraints highlights the importance of selecting the appropriate technology for specific distillation applications.

In addition, electrifying distillation faces notable challenges due to the mismatch between the stable energy demands of distillation and the fluctuating nature of renewable power generation. Although energy storage systems within utility infrastructure could, in theory, provide a stable renewable electricity supply, current electricity storage technologies are costly and lack sufficient capacity for large-scale industrial use.[14] The variability of renewable energy in the grid results in fluctuations in electricity supply and dynamic market pricing, sometimes even leading to negative prices. This creates an opportunity to operate distillation columns at a lower cost.

As the energy landscape becomes more dynamic, the concept of process flexibility has emerged as a crucial factor. Process flexibility refers to the ability of chemical processes to adjust power consumption in response to fluctuations in electricity availability and pricing.[15–17] This adaptability not only offers economic benefits by taking advantage of lower electricity prices but also helps maintain operational efficiency under variable power supply conditions. In power-to-X processes, process flexibility has demonstrated cost reductions of 20%–30% and improvements in efficiency.[15,18–20] However, these studies were conducted at the system level, assuming inherent flexibility without addressing detailed process designs to implement it. In reality, plenty of chemical processes, especially distillation, have limited operational flexibility due to constraints on load adjustments tied to mass transfers within the process.[21] Despite these challenges, early research has explored ways to enhance process flexibility through electrification and integration with energy and material storage. Wajeh et al. designed a flexible biodiesel production process by electrifying the distillation reboiler and incorporating intermediate and final buffer tanks, resulting in energy savings of up to 29%.[22] Similar strategies were applied to $CO_2$ capture processes, where electrification via heat pumps and solvent storage integration achieved 15% cost savings.[23,24]

In the literature, air separation units (ASUs) have been extensively studied for operational flexibility, largely because they are electricity-intensive processes that can readily be integrated with the grid for demand-response programs.[25,26] Caspari et al. proposed a flexible ASU design incorporating reflux liquid storage and an additional refrigeration unit, enabling a broad operational range from 3.5 to 28 MW.[27] An economic model predictive control applied to this flexible ASU yielded a 14% increase in economic benefits.[28] While enhancing flexibility in distillation processes is recognized as a key strategy, most studies have focused on ASUs, which are already fully electrified systems. There is a clear gap in both the literature and industrial practices regarding the development of a generalized flexibility design strategy applicable to conventional steam-driven distillation. Addressing this gap is essential, as the question of how to achieve operational flexibility in these systems—along with the development of corresponding design and operational strategies—remains unresolved. This highlights the need for innovative distillation designs that can adapt to fluctuating electricity supplies and pricing while preserving operational efficiency and economic feasibility.

This article introduces a first-of-a-kind approach for generalized distillation processes, designed for load adaptability and flexible operation in alignment with dynamic electricity markets shaped by the growing integration of renewable energy. The approach features a flexible electrified distillation system that utilizes flash vapor circulation (FVC) (a modification of MVR) for both electrification and adaptable operation, integrated with thermal storage to enable energy storage and management, resulting in exceptional operational flexibility. By integrating thermal storage, the system can act as a buffer against fluctuations in renewable power supply, allowing distillation to operate with zero electricity consumption, regardless of external energy conditions. To the best of the authors' knowledge, this is the first approach to propose flexible operation and energy storage for generalized steam-driven distillation systems. This represents a major advancement in distillation technology, offering a solution that not only aligns with the goals of decarbonization but also addresses the operational challenges associated with dynamic electricity markets and fluctuating renewable energy supplies. A case study on methanol/water distillation demonstrates the feasibility of this approach using two typical electricity pricing scenarios. The article also presents a systematic design and operational strategy for this flexible distillation system, along with mathematical models for simultaneous design and scheduling optimization, highlighting its economic benefits under various scenarios.

The structure of this article is organized as follows: Section 2 introduces the mechanisms and design concepts, including the FVC and thermal storage, for achieving load-adaptable distillation processes. Section 3 provides technical insights into the design of the FVC and thermal storage using a methanol/water example, analyzing

key factors influencing performance. Based on this analysis, Section 4 outlines the mathematical models for the simultaneous design and scheduling of the proposed distillation approach under two typical electricity pricing scenarios. Section 5 presents the optimization results and economic analysis. Finally, Section 6 concludes with key findings, limitations, and future recommendations.

## 2 | OVERVIEW OF THE APPROACH

### 2.1 | Load-adaptable distillation approach

The proposed load-adaptable distillation approach begins by electrifying the distillation process using heat pumps. These heat pumps upgrade the low-temperature waste heat in the overhead vapor to drive the reboilers.[29,30] However, existing heat pump-assisted distillation cannot adjust power consumption in response to fluctuating energy supplies or dynamic electricity markets. Therefore, this study proposes an innovative, load-adaptable distillation approach with the following key features.

1. *Electrified distillation with FVC*: The conventional steam-driven distillation column is integrated with an FVC system for electrification and load-adaptable operation, featuring a flash drum and vapor circulation. The FVC enables the variable generation of useful heat through flexible vapor circulation, controlled by compression pressure and condensation temperature, allowing for energy management and storage.
2. *Flexible power consumption*: With the implementation of FVC, the electricity usage can be flexibly adjusted by manipulating the vapor circulation rate, without prominently affecting the operational dynamics of the distillation column. The variation in electricity consumption enables operational flexibility when coupled with dynamic electricity markets or fluctuating energy supplies.
3. *Thermal storage mechanism*: A thermal storage system is designed to store the heat generated by the FVC, and the stored heat is used to drive the reboiler, in which cases the FVC is bypassed and electricity consumption is reduced to zero. Water is used as a storage medium for its high thermal capacity (compared to most fluids and suitable for days-long storage), easy availability (with potential reuse from the steam utility), and non-hazardous nature.

Two operational modes when coupled with dynamic electricity markets are shown in Figure 1. During off-peak periods, the distillation column operates at higher electricity consumption (off-peak operational mode) to store thermal energy, taking advantage of low electricity prices. The FVC is active, compressing the overhead vapor and generating heat. A portion of this heat is used to drive the reboiler, while the excess is stored in the thermal storage. During peak periods, the distillation column operates without electricity consumption (peak operational mode). The overhead vapor condenses conventionally, the FVC is off, and the boilup vapor is supplied using the heat from the thermal storage. By switching between two modes, the distillation process achieves flexibility and can adapt to dynamic electricity markets.

### 2.2 | Flash vapor circulation

The design and analysis of the FVC are presented. Initially proposed by the authors as an alternative to mechanical vapor recompression (MVR), the FVC is designed to fully electrify distillation processes.[31]

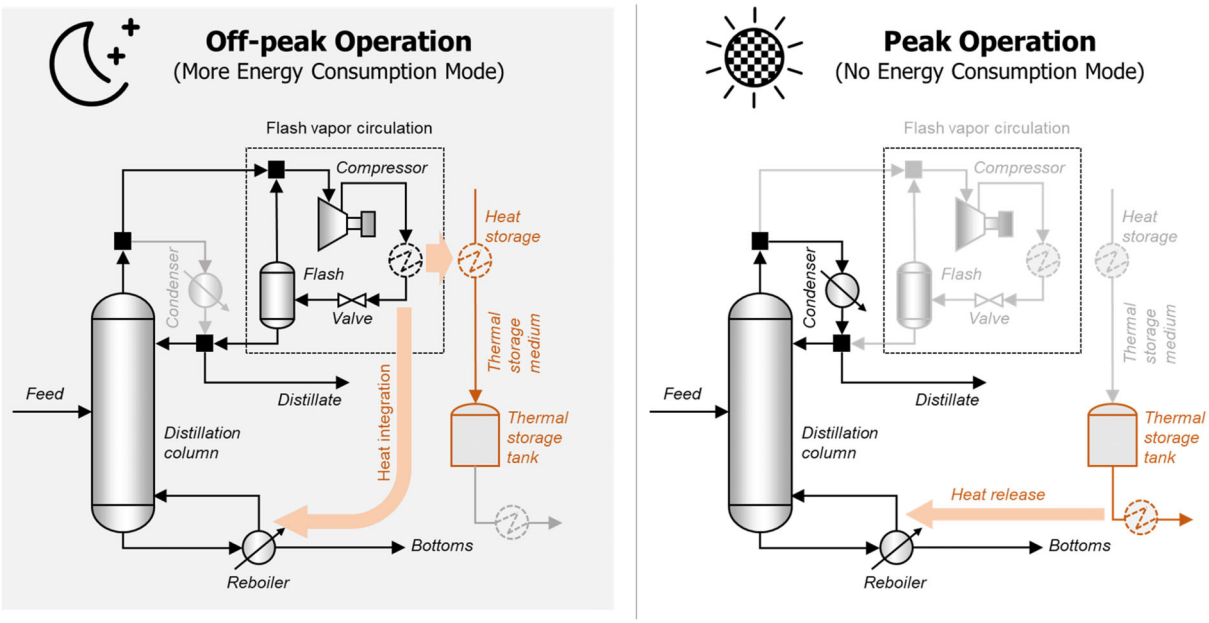


**FIGURE 1** Proposed approach for load-adaptable distillation.

Vapor circulation within the FVC not only satisfies the reboiler's heat demands but also generates additional heat through the compressor. The FVC has operational limits related to the maximum compression ratio and the outlet temperature of the compressor, which need to be controlled to ensure safety. To safely operate at high pressures, multi-stage compressors with inter-stage heat exchangers should be employed. The amount of additional heat that can be generated and the efficiency of this process are the two main aspects required to be considered in the FVC, which are measured by the COP of the heat pump. The COP is defined as the ratio of the heat output to the electricity input.

Figure 2 illustrates possible configurations of the FVC, which are primarily distinguished by the use of a multistage compressor and the location of vapor circulation. A comparison and analysis of these FVC configurations is necessary to identify the one with better performance. Considering the economic and complexity factors of the FVC, it is assumed that a compressor with no more than three stages is used. For vapor circulation, the pressure should match the inlet pressure of the corresponding stage of the compressor. Therefore, if the vapor circulation occurs at the first stage, the flash pressure should be the same as the column top pressure. Otherwise, the pressure will be higher than the column pressure, necessitating an additional valve and cooler to reduce the pressure and condense any vaporized fraction of the reflux. Additionally, in scenarios involving a three-stage compressor, vapor circulation to the third stage is not considered because an exceptionally high pressure may be required which can lead to safety issues and potentially insufficient heat generation due to a low vapor circulation rate. Inter-stage heat exchangers are installed to provide heat to the reboiler. Two heat exchangers are placed after the last stage: the first one supplies heat for storage, and the second one provides the remaining heat to the reboiler. The reason for supplying heat to storage via the first heat exchanger is that it operates at a higher temperature, allowing for a larger temperature difference in the thermal storage cycle, which reduces the amount of thermal storage medium required. Consequently, the temperature and pressure of the stream ($a$, $a3$, and $a4$, respectively) before the valve are two critical parameters that determine the FVC performance.

## 2.3 | Thermal storage

The storage of compression heat in the thermal storage system is crucial for managing the transition between off-peak and peak operations, which is commonly used in the design of Carnot battery systems.[32] In distillation, this process can be achieved through two methods: direct and indirect thermal storage, which are illustrated in Figure 3. In the indirect method, heat is transferred from the thermal storage medium to the reboiler. This method requires retrofitting the existing device to be heated by the thermal medium during peak operations. Pressurized water can be used as a thermal storage medium because of its high heat capacity, affordability, safety, and compatibility with existing steam utility systems. With a pressure of 20 bar, the boiling point of water can reach up to 212°C. This allows the stored water to remain in the liquid phase while providing the sensible heat for distillation processes, typically requiring temperatures below 200°C, particularly for hydrocarbons separation.

The direct method of heat storage involves pumping the bottom stream to high pressure, where it directly absorbs heat from the FVC. This heated bottom stream thus serves as the thermal storage medium in its liquid form. To recover energy, the stored liquid is depressurized through a valve to the bottom pressure, causing a fraction to vaporize. This vapor is then directed back to the column, providing the necessary boilup vapor. The remaining liquid fraction constitutes the bottom product. One distinct advantage of the direct method is the direct heat transfer between the medium and bottoms, which minimizes thermal energy losses. However, a notable

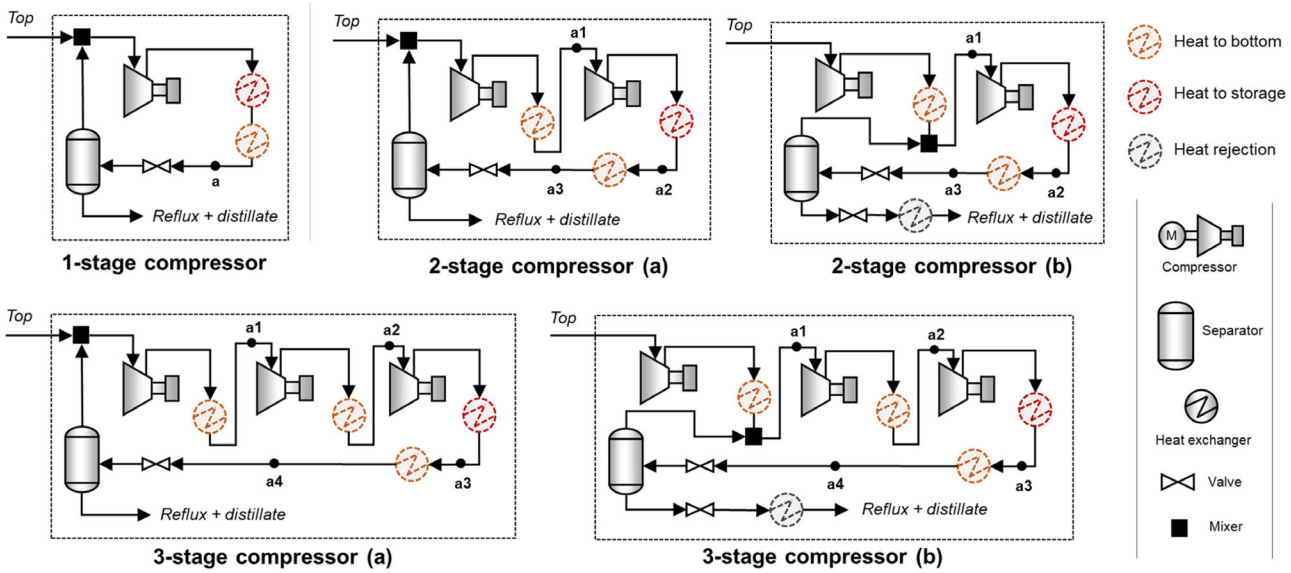


**FIGURE 2** Possible configurations of the FVC.

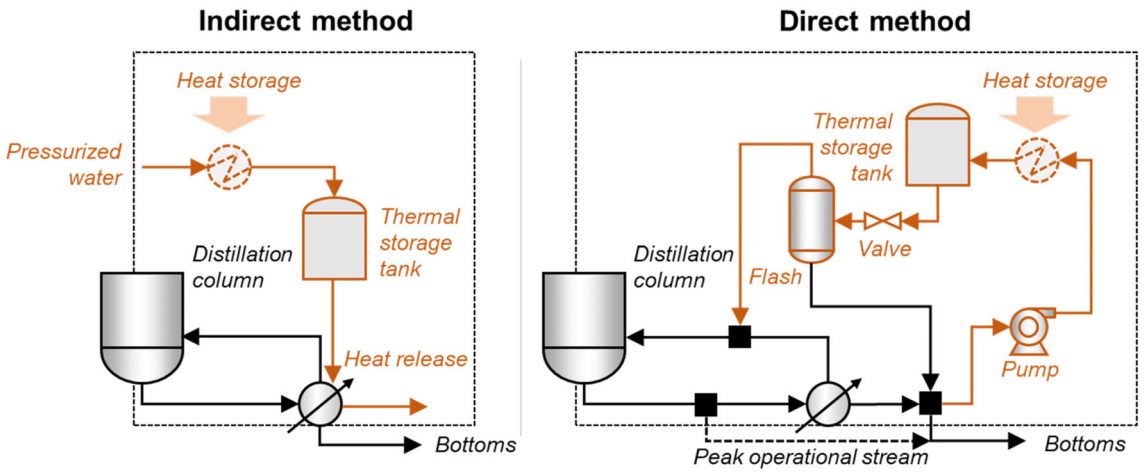


**FIGURE 3** Indirect and direct methods for thermal storage.

disadvantage is the inconsistent production of the bottom product. Specifically, during off-peak periods, the bottom product is utilized for thermal storage, which could potentially influence subsequent processes if the bottom product is required as feedstock to continuously feed to the subsequent process. In this case, an intermediate product tank is needed to stabilize the bottom production. During peak periods, the liquid drawn from the bottom is directly used as the product, since there is no need for reboiling to produce vapor for returning to the column; the returning vapor is supplied directly from the thermal storage. In this situation, the liquid product from the column may be off-specification, as it bypasses the reboiler (equivalent to the loss of one theoretical tray). However, the liquid from the flash is above the quality specification, as it undergoes an additional flashing process (equivalent to the gain of one theoretical tray). The mixture of these two liquids should balance the mole fraction of the bottom product to meet the predetermined separation specifications. Therefore, it is assumed that there will be no significant impact on the liquid product quality.

Given the approach and possible configurations for both the FVC and thermal storage, detailed design and optimization are presented using a motivating example to demonstrate the feasibility of the proposed approach.

## 3 | MOTIVATING EXAMPLE

### 3.1 | Methanol/water separation

Methanol/water separation through distillation is a crucial process, particularly in the context of using methanol as a renewable energy carrier.[33] Methanol can be synthesized from hydrogen, which is obtained by water electrolysis, and $CO_2$. This process is referred to as power-to-methanol where renewable electricity serves as the primary energy source, aligning with the background of the proposed approach.[34] The distillation column has 40 theoretical stages including the condenser and the reboiler, where the feed, consisting of methanol and water in molar fractions of 0.55 and 0.45 respectively, enters at the 30th stage at a flow rate of 100 kmol/h, temperature of 50°C, and pressure of 5 bar. The column operates at atmospheric pressure with a stage pressure drop of 0.7 kPa, producing high-purity products of 99.8 mol% methanol and 99.9 mol% water.

The modeling of a methanol/water distillation column was performed in Aspen Plus V14 using the NRTL property method. A reflux ratio of 0.4 is required to meet the separation criteria. The condenser and reboiler duties ($Q_{cond}$ and $Q_{reb}$) were calculated to be 1071 and 1167 $kW_{th}$, respectively. Vapor temperatures at the top and bottom of the distillation column were calculated at 64.6 and 106.8°C, respectively. A comparison was conducted between MVR and FVC designs to highlight the advantages of the FVC under identical separation conditions. The simulation employed several assumptions: (1) the compressor has an isentropic efficiency of 75%, (2) pressure drops throughout the FVC and thermal storage are considered negligible, and (3) a minimum temperature approach of 10°C is maintained in the heat exchangers.

Figure 4 compares the steady-state designs for conventional, MVR, and FVC distillation systems using one-stage or two-stage compressors. In the MVR design, the one-stage compressor outlet pressure is set at 8.87 bar to meet the reboiler's heat demand, while the FVC design only requires 5.86 bar, reducing power consumption to 285 $kW_e$ compared with 295 $kW_e$ in the MVR design. In MVR, 200 $kW_{th}$ of heat is wasted, which is then recovered through vapor circulation in the FVC, delivering 190 $kW_{th}$ of useful heat to storage. The same pattern holds for two-stage compressor designs, where both MVR and FVC have the same electricity consumption and heat output as their one-stage counterparts, though the two-stage MVR design requires a higher compressor outlet pressure of 9.2 bar. These results show that FVC outperforms MVR in terms of power efficiency and heat utilization, regardless of the number of compressor stages. The COP of the FVC (4.76) is higher than that of the MVR (4.63). Given this separation task, FVC is the preferred option over MVR.

As for dynamic operation, if the MVR operates dynamically to increase its compression pressure for higher power consumption and heat generation, a significant portion of the generated heat must be

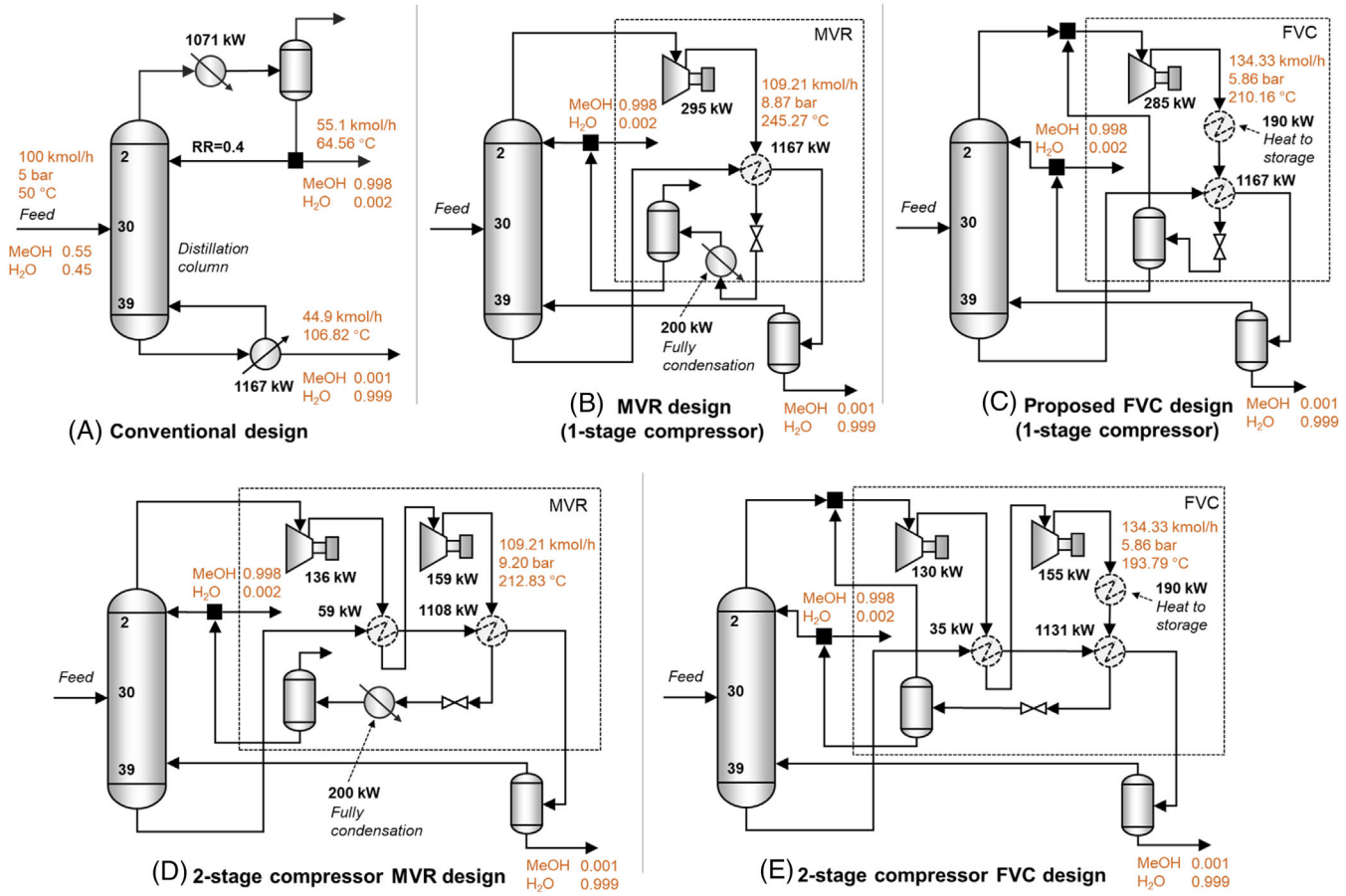


**FIGURE 4** Distillation designs for (A) conventional, (B) one-stage MVR, (C) one-stage FVC, (D) two-stage MVR, and (E) two-stage FVC.

rejected using cooling water to ensure complete condensation of the top product and prevent any vapor formation in the separator. In this case, the MVR is not suitable for flexible operation or for integrating thermal storage. In contrast, the FVC system recovers the rejected heat from the MVR system, enhancing overall efficiency and enabling thermal storage for later use in the reboiler.

## 3.2 | FVC design boundary

The temperature and pressure of streams *a*, *a*3, and *a*4 (as shown in Figure 2), hereinafter referred to as FVC's high temperature and pressure, are key parameters affecting the electricity consumption and heat output of the FVC. To explore the design boundaries, variations in these two parameters are examined for their impact on FVC's heat output (only for the heat to storage part) and COP in different configurations. The analysis includes two additional assumptions in the simulation: (1) The reflux pressure matches the operating pressure of the column, and (2) no constraints on compression ratio and outlet temperature for each compressor stage. The temperature range considered is from 117 to 200°C. The lower bound of 117°C accounts for the bottom temperature and a 10°C temperature approach, while the lower pressure bound is determined by the condensation pressure at 117°C, approximately 5.86 bar. The upper pressure bounds are set at 30, 50, and 80 bar for one-, two-, and three-stage compressor configurations, respectively. However, there is a case that the hot streams leaving the inter-stage heat exchangers at a high pressure become liquid at 117°C, thus it is invalid to enter the next stage compressor. In this case, the heat exchanger is specified as "hot stream outlet vapor fraction is 1" in the simulation, which corresponds to the pressure above 5.86 bar for the inter-stage stream. The detailed parameter ranges under investigation are listed in Table 1.

An initial screening of the possible FVC configurations was conducted under the ideal assumption that each compressor stage maintains an equal compression ratio, with the detailed procedure described in Appendix S1. The heat outputs and COPs for each configuration across the investigated temperature and pressure ranges are presented in Figures S5 and S6, and summarized in Table 2. As FVC's high temperature and pressure increase, heat output also increases. However, there is an infeasible region where certain combinations of FVC's high temperature and pressure are not feasible for its design. These infeasible regions were identified through simulation samples that indicated whether specific temperature and pressure combinations in the FVC were feasible. The results show that configurations with vapor circulation in the first stage, that is, configurations of one-stage, two-stage (a), and three-stage (a), achieved similar COPs across different compressor stage numbers, given the same heat output. Configurations (a) demonstrate significantly better performance,

**TABLE 1** Investigated temperature and pressure ranges.

| Parameter | One-stage FVC | Two-stage FVC | Three-stage FVC |
|---|---|---|---|
| Temperature range (°C) | 117–185[b] | 117–200 | 117–200 |
| Pressure range (bar)[a] | 5.86–30 | 5.86–50 | 7.4[c]–80 |

[a]Different simulation specifications were used for the inter-stage heat exchangers: the hot stream outlet temperature is set to 117°C when the pressure is below 5.86 bar, otherwise, the hot stream outlet is specified with a vapor fraction of 1.
[b]Maximum feasible temperature for one-stage configuration is 185°C.
[c]Minimum feasible pressure for three-stage configurations is 7.4 bar.

**TABLE 2** Summary of the initial screening results assuming equal compression ratio.

| Configuration | Min and max heat output ($kW_{th}$) | Min and max power usage ($kW_e$) | COP range |
|---|---|---|---|
| One-stage | 189.8–939.3 | 285.2–1034.8 | 4.76–2.04 |
| Two-stage (a) | 189.1–1307.8 | 284.5–1403.2 | 4.77–1.76 |
| Two-stage (b) | 64.3–479.2 | 284.5–803.9 | 4.33–2.05 |
| Three-stage (a) | 223.2–1495.5 | 328.6–1590.9 | 4.23–1.67 |
| Three-stage (b) | 132.5–827.5 | 289.9–1079.2 | 4.48–1.85 |

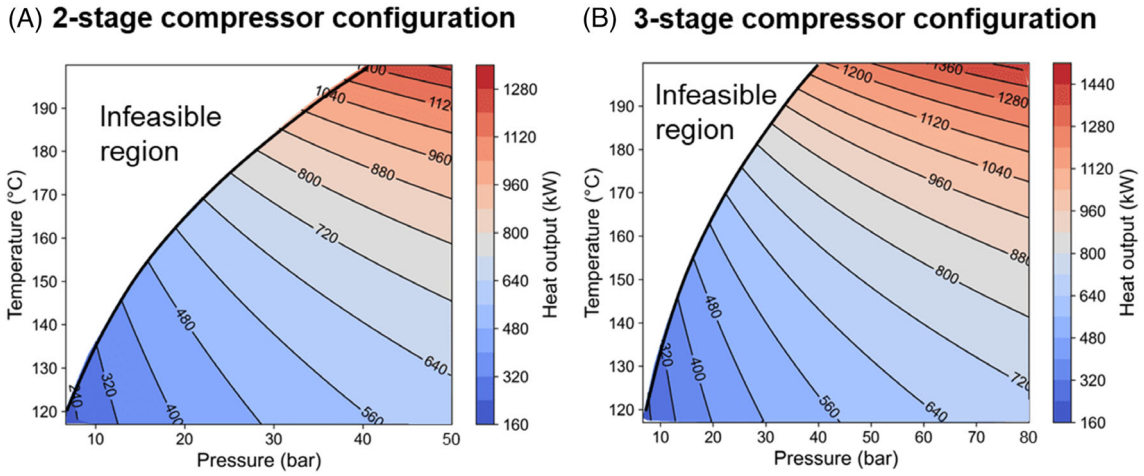


**FIGURE 5** Effect of FVC's high temperature and pressure on its heat output. (A) Two-stage compressor configuration; (B) three-stage compressor configuration.

providing both higher heat output and a higher COP for the same heat output compared to configurations (b) across all compressor stages. Additionally, increasing the number of compressor stages enhances the FVC's maximum heat output capacity: the three-stage compressor can deliver up to 1590 $kW_{th}$, while the one-stage and two-stage configurations peak at approximately 1000 and 1400 $kW_{th}$, respectively. On average, the FVC can provide between one-third and the full amount of heat required for the reboiler.

Further analysis is conducted for the two-stage and three-stage compressor configurations (a), as they are identified to have better performance compared to configuration (b). The results are shown in Figures 5 and 6.

The one-stage configuration is typically not considered due to its limited compression ratio in real-world applications. This time, the analysis was performed without the assumption of equal compression ratios. Instead, the compression ratio for each stage was optimized to maximize COP for a given final compression pressure based on sensitivity analysis. There is a trade-off between heat output and COP, with COP decreasing from approximately 4.7 at 200 $kW_{th}$ to 1.7 at 1400 $kW_{th}$, highlighting that higher heat output leads to reduced efficiency in the FVC. Notably, in both configurations, the same heat output corresponds to the same COP, as shown in Figure 6c,d. This suggests that regardless of the number of compressor stages, the COP is primarily determined by the heat output. Therefore, an optimization is needed to determine the optimal heat output, considering the potential decline in energy efficiency.

## 3.3 | Thermal storage analysis

In the indirect method of thermal storage, water is supplied at a pressure of 20 bar and a temperature of 117°C. This temperature

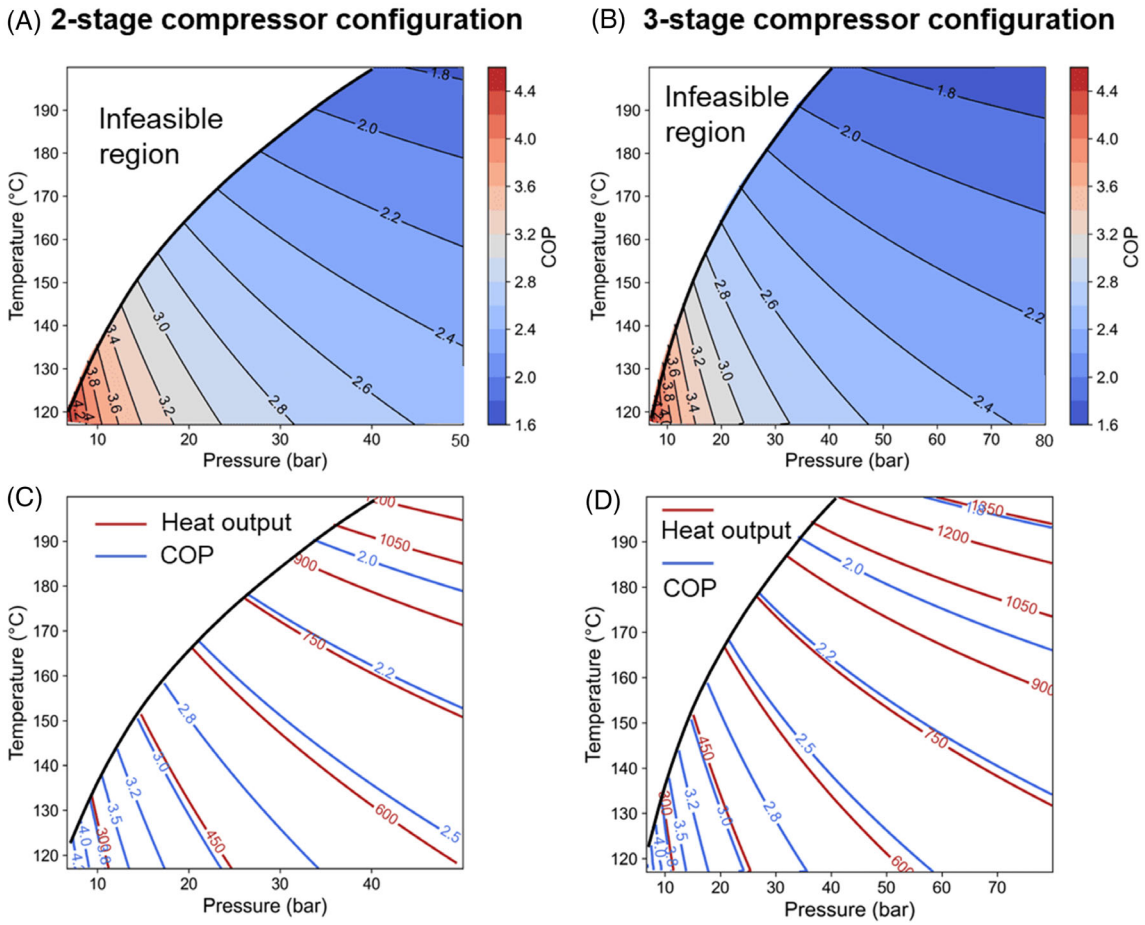


**FIGURE 6** Effect of FVC's high temperature and pressure on its COP. (A) Two-stage compressor configuration; (B) three-stage compressor configuration; (C) comparison between COP and heat output of the two-stage compressor configuration; (D) comparison between COP and heat output of the three-stage compressor configuration.

represents the minimum expected temperature of the return water after heat has been released during peak operation. The flow rate of water required for thermal storage is calculated based on the heat output from the FVC, taking into account the minimum temperature difference allowed in the heat exchanger used for heat storage. The thermal storage tanks are assumed to be ideally insulated and have no heat loss. Conversely, the direct method involves supplying water for thermal storage directly from the column bottom at a temperature of 107°C, where the bottom product is high-purity water. Owing to the lower temperature, a reduced water flow rate is anticipated compared to the indirect method. This water is also pressurized to 30 bar and the flow rate to the storage is determined by the minimum temperature difference in the heat exchanger when interfacing with the FVC. In the three-stage configuration, the water pressure for storage is increased to 40 bar to accommodate the higher top compression pressure of 80 bar.

Figure 7 illustrates the outcomes in relation to varying the FVC's high temperature and pressure. The results suggest that the direct method conserves around 40 kmol/h of water compared to the indirect method. However, the direct method requires about five to eight times the flow rate of the bottom product. Consequently, a product tank is necessary to hold sufficient bottom water when it is utilized for thermal storage. Importantly, when factoring in the required water flow, there is an optimal pathway for changing FVC's high pressure and temperature to raise heat output from low to high: first, raise the FVC's high pressure to 50 bar while maintaining the temperature at 117°C, and then increase the temperature while maintaining the pressure at 50 bar. Interestingly, as the heat output increases by raising the compressor pressure, the required water storage flow decreases due to the greater temperature difference in the heat exchanger, which is further caused by a higher compressor outlet temperature.

## 4 | DESIGN AND SCHEDULING OPTIMIZATION

During peak operation, the distillation column draws high-temperature water from the thermal storage tank, allowing it to operate only for a limited time until the storage reaches a minimum level. Optimal scheduling of the distillation column would balance the peak and off-peak operational modes, adjusting based on electricity price fluctuations and process dynamics. It should be noted that only the FVC-based distillation system is considered for flexible operation, as the MVR-based system is excluded due to its limited load-adjustment

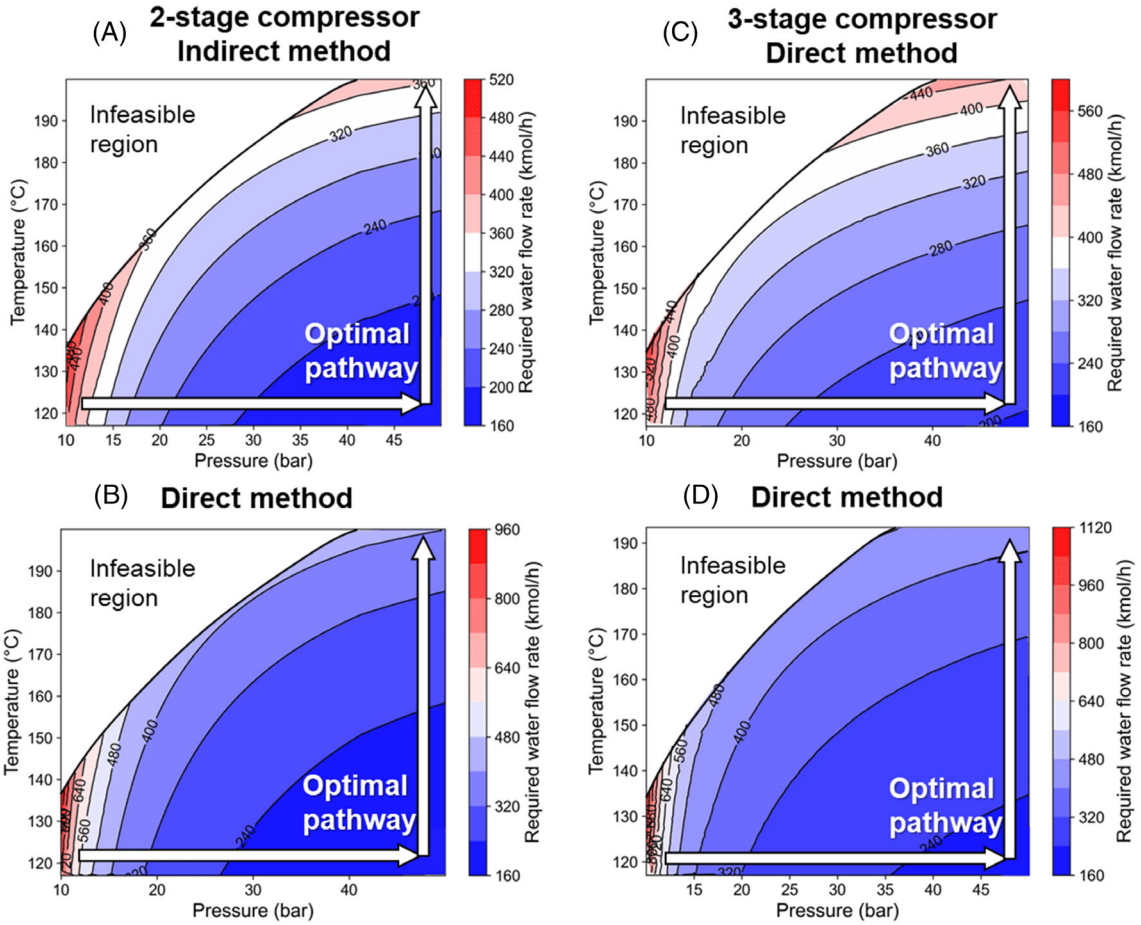


**FIGURE 7** Effect of FVC's high temperature and pressure on water flow rate for thermal storage. (A) Indirect method for two-stage compressor; (B) direct method for two-stage compressor; (C) indirect method for three-stage; (D) direct method for three-stage.

capability and lower efficiency. Therefore, the MVR system is typically operated in a steady-state under constant electricity prices.

## 4.1 | Problem definition

The optimal design and scheduling of the proposed distillation approach are closely linked due to its time-varying operation. This interdependence impacts the sizing of units involved in the dynamic operation (e.g., compressor, heat exchanger, and thermal storage tank) as part of the design decisions, as well as their operating modes (on/off status of the FVC and charging/discharging status of the thermal storage) and parameters. Traditionally, this is addressed by formulating a combined design and scheduling (CDS) problem, where operational decisions are explicitly incorporated into the design. However, this makes the optimization problem inherently large and computationally complex. In this study, the scheduling-informed design (SID) optimization method, proposed by Allman et al.,[35] is applied to overcome this challenge. The method first solves the scheduling problem using fixed design parameters, then leverages the optimal scheduling results obtained from a range of design parameters to solve the design problem, as illustrated in Figure 8.

## 4.2 | Optimization models

### 4.2.1 | Scheduling and storage constraints

In this study, simulation data from the FVC are used for design and operation optimization at an upper system level. At each time step, the optimal high temperature ($T_{FVC}$) and pressure ($P_{FVC}$) of the FVC must be determined, with the corresponding operating variables $Q_{str}$, $W_{str}$, and $F_{str}$, associated with each optimal condition pair. Based on the previously identified optimal pathway for increasing heat output in the FVC, $T_{FVC}$ and $P_{FVC}$ can be determined given $Q_{str}$, allowing $W_{str}$, and $F_{str}$ to be calculated accordingly. Thus, the relationships between these operating variables within the optimal pathway of the FVC can be effectively modeled using surrogate models to provide the mass and heat balances:

$$f_1(Q_{str}) = W_{str} \tag{1}$$

$$f_2(Q_{str}) = F_{str} \tag{2}$$

Here, $Q_{str}$ denotes the heat output ($kW_{th}$) for storage, $W_{str}$ stands for the power required ($kW_e$) for compression, and $F_{str}$ annotates the

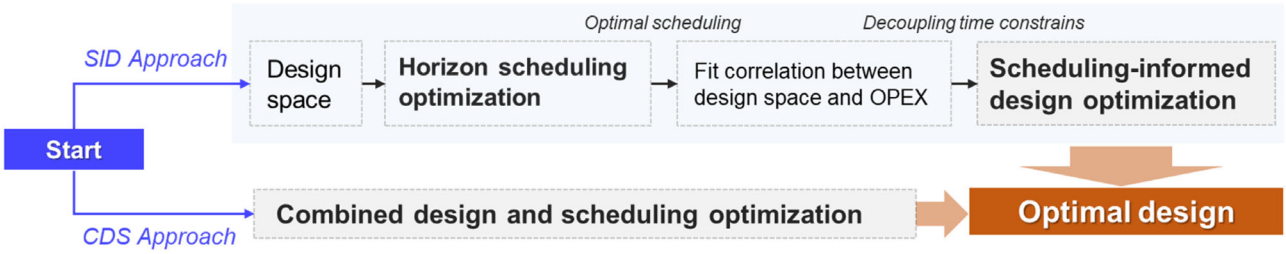


**FIGURE 8** Procedure for the combined design and scheduling optimization problem and the scheduling-informed design optimization problem.

required mole flow rate (kmol/h) of water for thermal storage. The surrogate functions $f_1$ and $f_2$ are derived using the ALAMO (automated learning of algebraic models for optimization) method,[36] which utilizes a set of basis functions of the input variables to build the surrogate models from Aspen simulation data. This approach ensures efficient optimization with reduced computational demands, utilizing the algebraic surrogate models. Detailed surrogate modeling is provided in Appendix S1.

The energy flows between the distillation column, FVC, and thermal storage tank are the physical bounds for the optimization, which are as follows:

$$E_{\text{tank}}(t) = E_{\text{tank}}(t-\Delta T) + Q_{\text{str}}(t)\cdot\Delta T - Q_{\text{rls}}(t)\cdot\Delta T \tag{3}$$

$$Q_{\text{rls}}(t) = Q_{\text{reb}}\cdot(1-\delta(t)) \tag{4}$$

where $E_{\text{tank}}$ and $Q_{\text{rls}}$ denote the stored energy ($kW_e h$) and thermal energy output ($kW_{th}$) from the storage tank, respectively. $\delta$ is a binary variable for which 1 represents the off-peak operational mode and 0 represents the peak operational mode of the distillation column, respectively. The time step size for the optimization, $\Delta T$, is set to 1 h, as the column units have high ramp rates and fast dynamics relative to the time step (1 h). This choice is based on several factors: (1) The dynamic components of the system (FVC and thermal storage) operate with faster dynamics than the column itself, with minimal impact on mass and heat transfer within the column. (2) The day-ahead electricity market updates prices hourly, aligning with the 1-h time step. (3) The 1-h interval strikes a balance between computational efficiency and optimization accuracy.

Therefore, quasi-stationarity is assumed at each operating point, meaning the distillation column is considered to be in a steady state at each time step, independent of the operating point from the previous time step. Additionally, further calculations are needed to account for the liquid holdup in the thermal storage tank, using the temperature correlation:

$$L_{\text{tank}}(t) = L_{\text{tank}}(t-\Delta T) + F_{\text{str}}(t)\cdot\Delta T - F_{\text{rls}}(t)\cdot\Delta T \tag{5}$$

$$F_{\text{rls}}(t) = \frac{Q_{\text{rls}}(t)}{c\cdot(T_{\text{tank}}(t) - T_{\text{btm}} - T_{\text{diff}})} \tag{6}$$

where $L_{\text{tank}}$ and $F_{\text{rls}}$ denote the liquid holdup (kmol) and released water flow rate (kmol/h) from the thermal storage tank, respectively. The released water flow is influenced by the temperature of the stored water, which can be described as follows:

$$\begin{aligned} &L_{\text{tank}}(t-\Delta T)\cdot(T_{\text{tank}}(t) - T_{\text{tank}}(t-\Delta T)) \\ &= F_{\text{str}}(t)\cdot(T_{\text{str}}(t) - T_{\text{tank}}(t))\cdot\Delta T\cdot\delta(t) \end{aligned} \tag{7}$$

$$T_{\text{str}}(t) = \frac{Q_{\text{str}}(t)}{c\cdot F_{\text{str}}(t)} + T_{\text{btm}} + T_{\text{diff}} \tag{8}$$

where $T_{\text{tank}}$, $T_{\text{str}}$, $T_{\text{btm}}$, and $T_{\text{diff}}$ represent the temperature of the stored water, the temperature of the water at the charging end, the bottom temperature of the distillation column, and the minimum temperature difference in the heat exchangers (10°C), respectively. $c$ is the specific heat capacity ($kW_{th}h/kmol/°C$) of water at the working pressure. It is important to note that an initial storage holdup is required for the optimization, with the initial tank temperature estimated as follows:

$$T_{\text{int}} = \frac{E_{\text{int}}}{c\cdot L_{\text{int}}} + T_{\text{btm}} + T_{\text{diff}} \tag{9}$$

where $T_{\text{int}}$, $E_{\text{int}}$, and $L_{\text{int}}$ represent the initial temperature, initial energy, and initial holdup of the thermal storage tank. In this study, the initial holdup is set to 15% of the storage capacity, and the initial energy is assumed to be half of the holdup value to estimate a reasonable initial temperature. Demonstrations of the operational modes and scheduling variables of the distillation system are provided in Figures 9 and 10, respectively.

The thermal storage is constrained by a physical limit that requires the storage holdup to remain below its maximum capacity, $L_{\text{cap}}$. Additionally, while the high temperature and pressure in the FVC can be varied to adjust the heat output, the heat exchanger has a maximum capacity, $Q_{\text{cap}}$, which the heat output to thermal storage must not exceed. Similarly, the compressor must be designed with a maximum power output capacity, $W_{\text{cap}}$.

$$0 \le L_{\text{tank}}(t) \le L_{\text{cap}} \tag{10}$$

$$0 \le Q_{\text{str}}(t) \le Q_{\text{cap}} \tag{11}$$

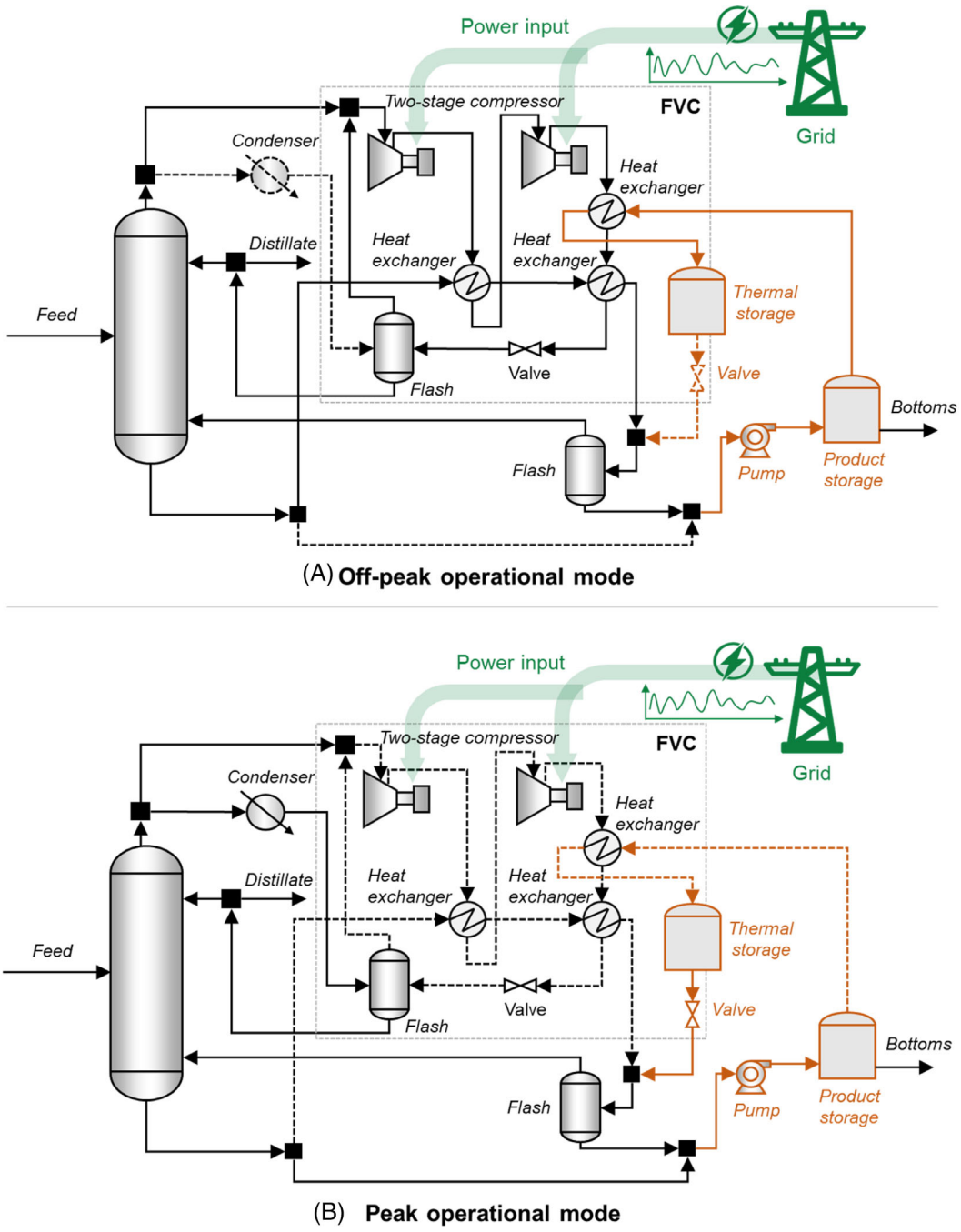


**FIGURE 9** Operational modes for the distillation system using a two-stage compressor.

$$0 \le W_{str}(t) \le W_{cap} \tag{12}$$

$$TAC = \frac{\theta(\theta+1)^{PL}}{(\theta+1)^{PL}-1} \cdot \sum_{i=1}^{N_{units}} CAPEX_i\left(L_{cap}, W_{cap}, Q_{cap}\right) + OPEX_{ele} + OPEX_{cooling} \tag{13}$$

### 4.2.2 | Cost modeling

The optimization considers the design capacities of the FAC and thermal storage, the change of high temperature and pressure in the FVC, and the switch between peak and off-peak operational modes for minimizing the total annual cost (TAC) of the distillation column taking advantage of electricity price fluctuations. The TAC is calculated as follows:

$$OPEX_{ele} = \sum_{t=1}^{8760} C_{ele}(t) \cdot W_{str}(t) \cdot \delta(t) \tag{14}$$

$$OPEX_{cooling} = \sum_{t=1}^{8760} C_{cooling} \cdot Q_{cond} \cdot (1-\delta(t)) \tag{15}$$

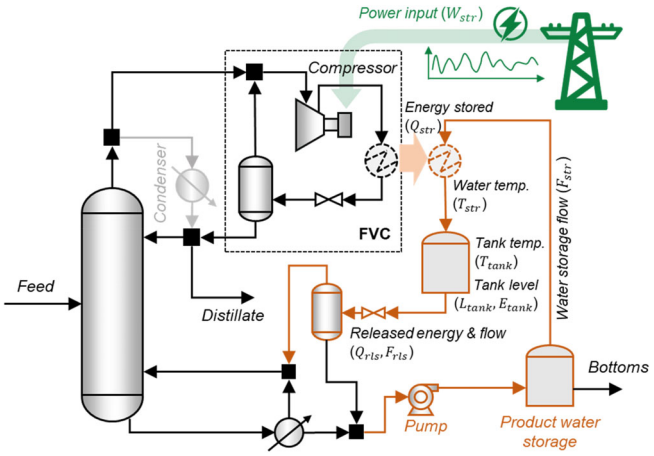


**FIGURE 10** Scheduling variables for the distillation system.

where $CAPEX_i$ represents the CAPEX of unit $i$ taking into account the unit size such as $L_{cap}$ for the storage tank, $Q_{cap}$ for the heat exchanger, and $W_{cap}$ for the compressor. OPEX denotes the annual OPEX which includes the annual electricity cost ($OPEX_{ele}$) and annual cooling cost ($OPEX_{cooling}$). $\theta$ is the interest rate (set as 8%), and PL is plant life (set as 25 years). Equipment such as pumps, valves, and the reflux drum are ignored at the conceptual design stage. Detailed CAPEX modeling of each unit of the distillation column and the FVC is provided in Appendix S1.

### 4.2.3 | Scheduling optimization problem

A 24-h receding horizon scheduling problem (P.1) is formulated to determine the operating states (on-/off-peak) and the scheduling of the units, taking into account the day-ahead electricity market. The term "horizon scheduling" refers to solving a dynamic optimization problem over a defined time horizon, using available forecasts for the next 24 h and the current system state to develop a scheduling strategy that minimizes OPEX over the 24-h period. Once solved, the actions for the first hour are implemented, forecasts are updated, and a new scheduling problem is solved based on the updated state and forecasts. This process repeats every hour throughout the operating period, and all costs incurred are accumulated to calculate the annual OPEX for the distillation system. Whole-period simulations are then conducted iteratively across the design space to establish correlations between annual OPEX and the design parameters. The scheduling problem P.1 is defined as follows.

$$\begin{aligned}\min.OPEX_{Hor} = &\sum_{t=1}^{24} C_{ele}(t)\cdot W_{str}(t)\cdot\delta(t) + C_{cooling}\cdot Q_{cond}\\ &\cdot(1-\delta(t)) + \zeta\cdot(E_{int} - E_{tank}(t=24))\\ \text{s.t. Equations}&(1)-(12)\end{aligned} \tag{16}$$

Here, $OPEX_{Hor}$ is the calculated OPEX over the 24-h period. $\zeta$ is the artificial penalty term for using the initial energy from the thermal storage, set to 0.01 in this study. The OPEX for the first time frame is recorded. Problem P.1 is a mixed-integer nonlinear programming (MINLP) model, consisting of 336 equations and 242 variables.

### 4.2.4 | Design optimization problem

OPEX correlations based on the installed capacities of size-varying units can be developed ($OPEX(L_{cap}, W_{cap})$ ) using the results from the scheduling optimization problem P.1. Thus, both capital and operating costs are functions of the installed capacities of the candidate units. It should be noted that using electricity price profiles from different years leads to different correlations for OPEX. These variations in electricity price profiles can affect the design optimization process. Therefore, the uncertainty associated with electricity prices from different years can impact the optimization results. However, this is outside the scope of the current study, as a fixed-period electricity price profile was used to determine the optimal design. The design optimization problem (P.2) can be defined as follows, based on Equation (13).

$$\begin{aligned}\min.TAC = &\frac{\theta(\theta+1)^{PL}}{(\theta+1)^{PL}-1}\cdot\sum_{i=1}^{N_{units}} CAPEX_i(L_{cap}, W_{cap}, Q_{cap})\\ &+ OPEX(L_{cap}, W_{cap})\ \text{s.t. Equations}\ (1)-(12)\end{aligned} \tag{17}$$

Problem P.2 is formulated as a nonlinear programming (NLP) model. Furthermore, when the distillation operation is aligned with predefined peak and off-peak periods with fixed electricity prices, the combined design and scheduling optimization problem (P.3) should be solved as an NLP model, since the integer variables in the original problem are removed. In this case, an additional constraint, as described in Equation (18), should be incorporated:

$$\delta(t) = \begin{cases} 1 & t \in \text{offpeak hours} \\ 0 & t \in \text{peak hours} \end{cases} \tag{18}$$

Problem P.3 can thus be defined as follows.

$$\begin{aligned}\min.TAC = &\frac{\theta(\theta+1)^{PL}}{(\theta+1)^{PL}-1}\cdot\sum_{i=1}^{N_{units}} CAPEX_i(L_{cap}, W_{cap}, Q_{cap})\\ &+ OPEX_{ele} + OPEX_{cooling}\\ \text{s.t. Equations}&(1)-(12),(18)\end{aligned} \tag{19}$$

## 4.3 | Electricity market scenarios and optimization implementation

The distillation column is assumed to be grid-connected, with no power availability limitations and no impact of energy exchange on electricity prices. Two representative electricity price scenarios were analyzed: one based on historical day-ahead electricity prices in the Netherlands for the first two months of 2022[37] (Scenario a) and another based on predefined peak and off-peak periods with fixed prices in Gansu province, China (Scenario b). Scenario a is typical of

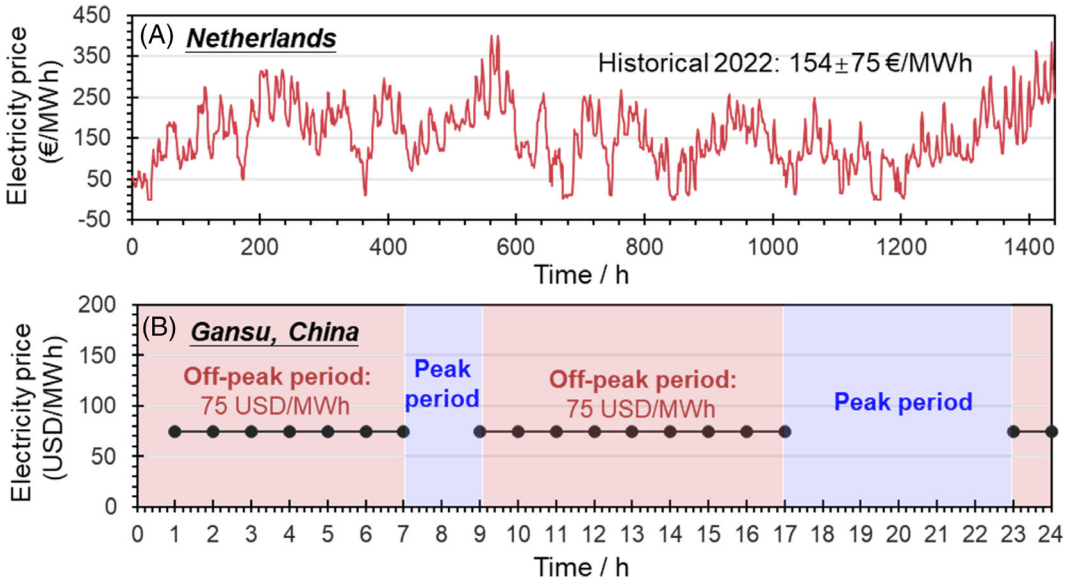


**FIGURE 11** Electricity price scenarios. (A) Two-month day-ahead electricity market in the Netherlands; (B) fixed electricity market in Gansu province, China.

grids with high renewable energy penetration, such as in Europe, while Scenario b represents grids with low to medium renewable penetration, as seen in China. As illustrated in Figure 11, the average electricity price in Scenario a is 154 €/MWh with a standard deviation of 75 €/MWh, while in Scenario b, the off-peak electricity price is set at 75 USD/MWh for 16 h per day, based on the local grid's electricity pricing and availability.[38] The peak electricity price is not displayed, as it is not used in the optimization.

Scenario a corresponds to the original optimization problems P.1 and P.2, where integer variables determine the operational mode for each time step. The scheduling optimization problem P.1 was solved over a two-month period, and the annual OPEX was extrapolated to a full year (8760 h), assuming that the annual OPEX is six times the OPEX over the two-month period. In Scenario b, distinct peak and off-peak periods are defined, with the FVC operating only during off-peak periods, reflecting optimization problem P.3. All problems (P.1–P.3) were solved using the DICOPT4 solver in GAMS in under 1min, thanks to DICOPT4's efficient handling of MINLP problems. By balancing solution quality with computational efficiency, DICOPT4 effectively manages both nonlinearities and discrete variables, allowing for fast convergence. This makes it particularly suitable for large-scale optimization problems and provides a practical alternative to global solvers, which would be computationally intensive in this case. However, other local solvers, such as CPLEX and Gurobi, can also be used in this case.

## 5 | OPTIMIZATION AND PERFORMANCE ANALYSIS

The proposed distillation approach is optimized under two scenarios, and the results are compared to the MVR-based distillation system, which is assumed to operate under constant electricity prices. This is because the MVR system is not suitable for flexible operation or for adjusting power consumption for energy management in response to electricity price fluctuations, as evidenced by previous discussions. Therefore, it does not participate in electricity market services.

### 5.1 | Effect of storage and compressor capacities

The scheduling optimization results in **Scenario a** are obtained under varying thermal storage and compressor capacities, showing a clear correlation between these design capacities and the resulting annual OPEX of the proposed distillation system. This relationship is illustrated in Figure 12, where the relative OPEX values are plotted against thermal storage capacity and maximum allowed compressor work (compressor capacity). A third-order polynomial function was used to fit these relationships, with trendlines and $R^2$ values mostly exceeding 0.98, indicating a strong fit. Both thermal storage capacity and maximum compressor work exhibit a strong correlation with OPEX. As storage capacity increases, OPEX decreases, but it levels off after 15,000 kmol, indicating that further increases beyond this point yield minimal reductions in OPEX. Additionally, increasing the maximum compressor work results in a near-linear decrease in OPEX, as indicated by the trendlines. These trendline equations are used to model the correlation between OPEX and the two design variables, which are then applied in the design optimization process. The design ranges considered include compressor work between 400 and 700 $kW_e$ and thermal storage capacity between 4000 and 17,000 kmol. A minimum compressor work of 400 $kW_e$ corresponds to approximately 300 $kW_{th}$ of heat output, below which the required water flow for storage increases significantly, as shown in Figure 7. This results in the need for large piping and equipment.

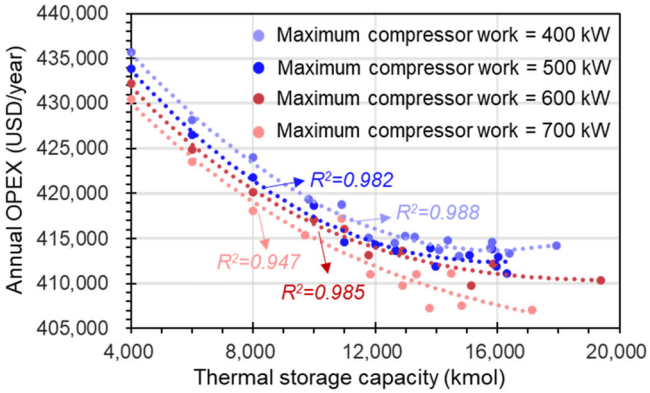


**FIGURE 12** Optimal annual OPEX under varying storage and compressor capacities.

## 5.2 | Design optimization of FVC and thermal storage in Scenario a

Using the correlated function between the design space (compressor and thermal storage capacities) and annual OPEX, the design optimization was solved for Scenario a. Specifically, the two-stage compressor configuration is included in the optimization, with the design range for compressor work set between 400 and 700 $kW_e$. The optimal design resulted in a compressor capacity of 400 $kW_e$ and a thermal storage capacity of 13,246 kmol (approximately 303.2 $m^3$), with the compressor capacity reaching the minimum limit of the considered design range. This optimal design was then compared to the MVR system, which is based on a two-stage compressor, under the assumption that the MVR operates at a fixed electricity price ranging from the average price in Scenario a (154 €/MWh) to a higher value of 180 €/MWh. Figure 13a presents the annual OPEX comparison, showing that the MVR's OPEX is 6.1% higher than the FVC's at the average electricity price. Additionally, when the electricity price for constant use in the MVR increases from 154 to 180 €/MWh, the OPEX of the MVR rises sharply, up to 23.9% higher than the FVC's. This highlights the cost-saving potential of flexible operation under fluctuating electricity markets. Figure 13b,c displays the CAPEX and TAC comparisons for MVR and FVC distillation systems. In both cases, the compressor is the most expensive component, accounting for over 68% of the CAPEX. The cost shares for heat exchangers and the distillation column are similar, while the thermal storage contributes the least, only 7.8% of the total CAPEX for the FVC. The lower cost of thermal storage supports the viability of the proposed approach for coupling with dynamic electricity markets. However, the high CAPEX of the compressor poses a challenge, limiting the cost benefits of flexible operation. Consequently, the TAC of the FVC is slightly higher than that of the MVR at the average electricity price. Nonetheless, if electricity prices increase to 180 €/MWh, the FVC shows cost advantages due to the substantial reduction in OPEX.

The scheduling results under the optimal design for Scenario a provide insights into system operation. Figure 14a,b displays the storage holdup profile for a selected time period (49th to 96th hour) and over a two-month period, respectively. The storage holdup fluctuates between zero and the tank's maximum capacity, demonstrating that thermal storage effectively balances the heat demand of the distillation column. The FVC's on and off status is clearly visible in the zoomed-in period, with the FVC operating primarily during periods of decreasing electricity prices, especially after the 20th hour. The system is optimally scheduled to capitalize on lower electricity prices by storing heat produced by the FVC. Conversely, the FVC shuts off, and the distillation column relies on stored heat during periods of high electricity prices. Figure 14c illustrates the tank temperature profile, where the temperature initially rises and stabilizes at around 146°C, reaching near-equilibrium between water charging and discharging operations. This temperature is optimal for safe storage and minimizes energy loss due to heat transfer to the environment. The initial temperature increase is due to the lower starting temperature, determined by the initial condition of the thermal storage tank. Different initial tank conditions could have a notable impact on the system operation and performance.

## 5.3 | Design optimization of FVC and thermal storage in Scenario b

For Scenario b, the design and scheduling problem was solved to determine the optimal design, using the same compressor work and thermal storage design ranges as in Scenario a. The optimal design resulted in a 679 $kW_e$ compressor capacity and 1956 kmol thermal storage capacity (approximately 44.8 $m^2$). Compared to Scenario a, the optimal design in Scenario b requires a larger compressor capacity but a significantly smaller storage capacity. This design was also compared with the MVR based on a two-stage compressor, under the assumption that the MVR operates at a fixed electricity price ranging from 115 to 150 USD/MWh. Figure 15a presents the OPEX comparison across different electricity prices. Additionally, various off-peak electricity prices were considered for the FVC, ranging from the base case of 75 USD/MWh to 100 and 125 USD/MWh. When the electricity price for the MVR reaches 115.3 USD/MWh, the FVC's OPEX is lower, demonstrating its cost advantage when the electricity price exceeds 115.3 USD/MWh. In real-world scenarios, electricity prices fluctuate based on the local market, but the all-time fixed electricity price is typically more than 1.5 times the off-peak price, which is above 112.5 USD/MWh. This suggests that in most cases, the FVC can reduce OPEX during operation. If the all-time fixed electricity price rises to 200 €/MWh, the OPEX of the MVR significantly increases, reaching up to 90.1% higher than that of the FVC. By adjusting the off-peak electricity price, the minimum all-time fixed electricity prices at which the FVC retains its OPEX advantage are 153.5 and 191.8 USD/MWh, corresponding to off-peak prices of 100 and 125 USD/MWh, respectively. Generally, the FVC maintains its OPEX advantage when the all-time fixed electricity price is at least 1.5 times higher than the off-peak price.

Figure 14b,c presents the CAPEX and TAC comparisons between the MVR and FVC distillation systems. In Scenario b, the compressor

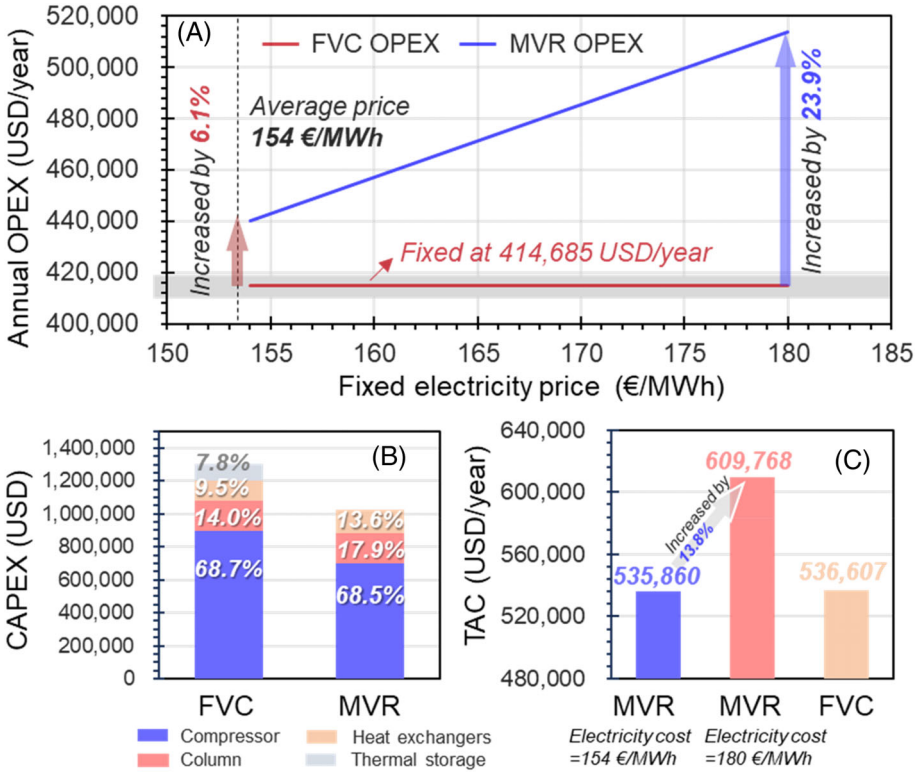


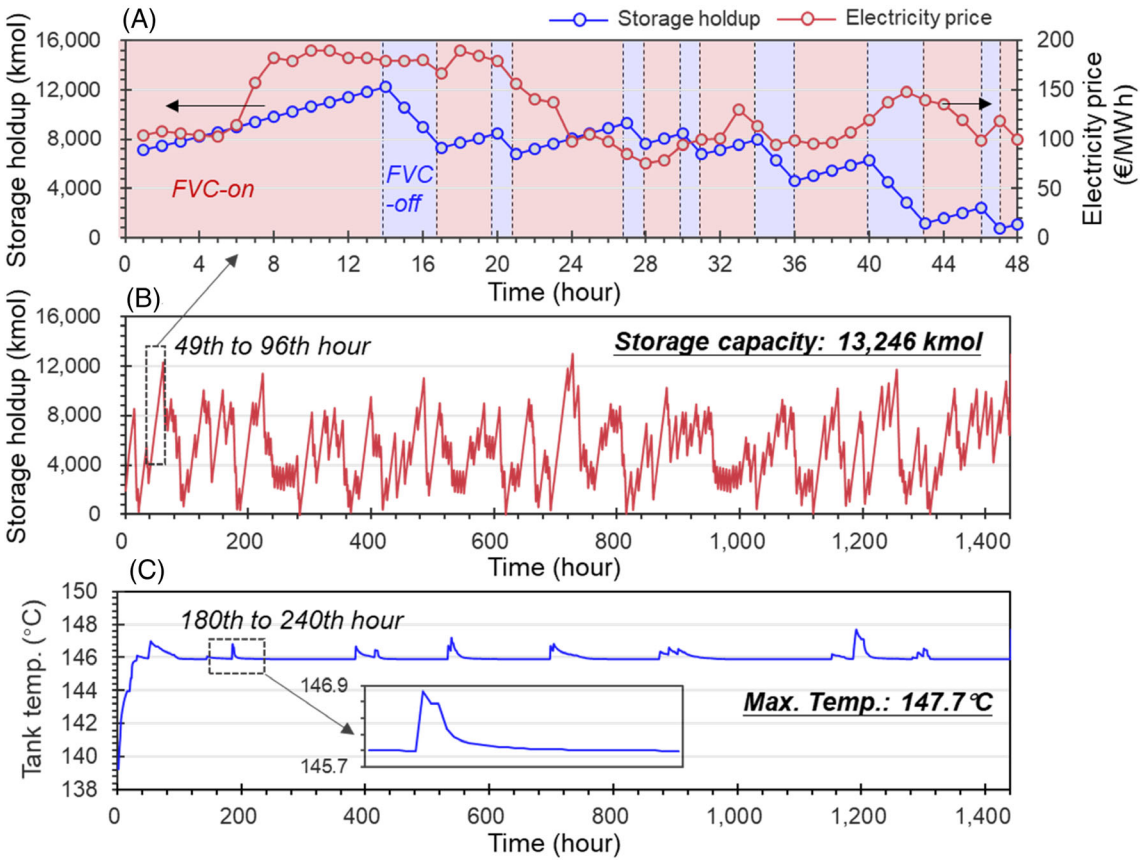


**FIGURE 13** Cost comparison between the MVR and FVC for Scenario a. (A) OPEX comparison; (B) CAPEX comparison; (C) TAC comparison.

**FIGURE 14** System scheduling under the optimal design for Scenario a. (A) Storage holdup profile for a selected time period (49th to 96th hour); (B) storage holdup profile over a two-month period; (C) tank temperature profile over a 2-month period.

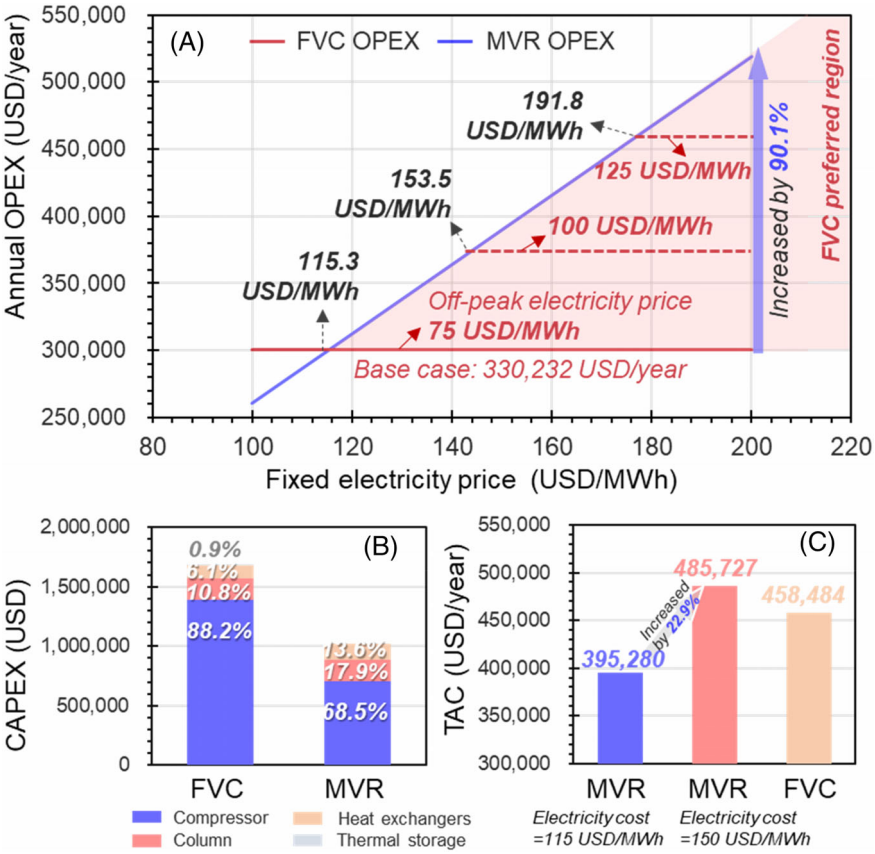


**FIGURE 15** Cost comparison between the MVR and FVC for Scenario b: (A) OPEX comparison; (B) CAPEX comparison; (C) TAC comparison.

accounts for a larger portion of the CAPEX (88.2%) compared to Scenario a, due to the increased demand for compressor work. The CAPEX for heat exchangers slightly decreased, as the increased compressor outlet temperature allowed for a greater temperature approach. With greatly reduced thermal storage capacity, the thermal storage contributes only 0.9% of the total CAPEX for the FVC. As a result of the higher compressor CAPEX, the TAC for the FVC is also higher. In the base case with an all-time fixed electricity price of 115 USD/MWh, the FVC offers no economic advantage. However, the FVC becomes competitive when the fixed electricity price is double the off-peak price, which is common in many regions with high penetration of renewables. Therefore, the FVC still holds economic potential in scenarios where the off-peak electricity price is very low and significantly different from normal or peak prices.

From the storage holdup profile for the first 48 h shown in Figure 16 (1000 kmol approximates to 23 $m^3$), the FVC operates periodically, cycling from zero holdup back to zero over a 24-h period, in response to the electricity price, which also changes periodically. For balanced operation within 24 h, a high charging rate is required, leading to a greater demand for compressor work. However, this balanced operation, along with the low required water storage flow caused by a high compressor work, reduces the need for long-period thermal storage compared to Scenario a, highlighting a design trade-off between requiring a larger compressor (Scenario b) and a larger thermal storage tank (Scenario a). This, in turn, results in a trade-off between the high CAPEX of the compressor and the high CAPEX of the storage tank. It is important to note that the total duration of peak and off-peak periods within a day affects scheduling, influencing the charging rate and the optimal design. A shorter off-peak period increases the charging rate, necessitating a larger compressor capacity. Additionally, the water storage temperature rises, with the current scenario maintaining a constant tank temperature of 268°C due to a steady charging rate throughout the operation period. This temperature is considerably higher than in Scenario a, indicating the need for minimizing energy losses and ensuring the safety of thermal storage.

## 5.4 | Effect of compressor cost model

Given that compressor cost is the most significant factor influencing the optimal design and economic performance of the proposed distillation approach, an investigation was conducted to compare the optimal results using different compressor cost models. Luyben reviewed various published models for estimating compressor costs and found that different models yield substantial variations in compressor costs, introducing uncertainty even for conceptual design evaluations.[39] A total of eight cost modes, listed in Table 3, are available for estimating the purchase cost of centrifugal and reciprocating compressors, both of which can be used in the FVC. Two cost indexes, the Chemical Engineering Plant Cost (CE) Index and the Marshall-Swift Equipment Cost (MS) Index, were used to update the costs to the recent CE index of 800 and MS index of 1975.8.

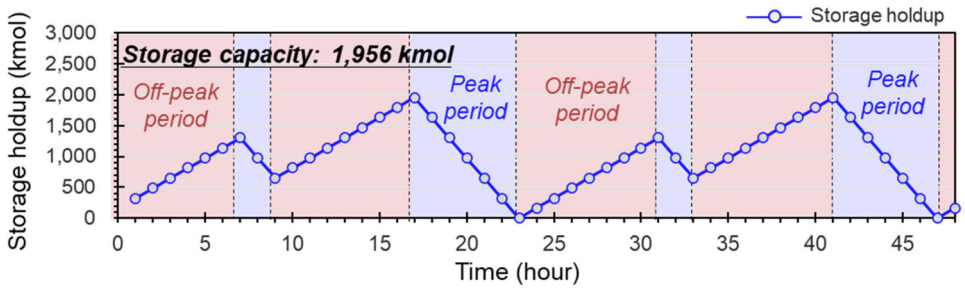


**FIGURE 16** Storage holdup profile under the optimal design for Scenario b.

**TABLE 3** Summary of compressor cost models.

| Author | Cost equation (s) | Cost index | Note |
|---|---|---|---|
| Douglas[40] | $CAPEX_{comp} = 5840 W_{cap}^{0.82}$ | - | Base case, no specific compressor type |
| Turton et al.[41] | $CAPEX_{comp} = 10^{2.2897+1.3604\log_{10}(W_{cap})-0.1027[\log_{10}(W_{cap})]^2}$ | CE = 397 | For both centrifugal and reciprocating types |
| | $CAPEX_{drives} = 10^{2.9508+1.0688\log_{10}(W_{cap})-0.1315[\log_{10}(W_{cap})]^2}$ | | - |
| Peters and Timmerhaus[42a] | $CAPEX_{comp} = 315 W_{cap} + 13{,}000$ | MS = 904 | For centrifugal type |
| | $CAPEX_{comp} = 430 W_{cap} + 16{,}000$ | | For reciprocating type |
| Seider et al.[43] | $CAPEX_{comp} = \exp[9.1553 + 0.63\ln(W_{cap})]$ | CE = 567 | For centrifugal type |
| | $CAPEX_{comp} = \exp[4.6762 + 1.23\ln(W_{cap})]$ | | For reciprocating type |
| Ulrich[44a] | $CAPEX_{comp} = 315 W_{cap} + 13{,}000$ | CE = 315 | For both centrifugal and reciprocating types |
| Luyben[39] | $CAPEX_{comp} = 2.5\exp[7.58 + 0.8\ln(W_{cap})]$<br>$CAPEX_{motor} = 2049 + 668.16 W_{cap}$ | - | No specific compressor type |

[a]Self-fitted equations within the specified design range.

The compressor cost models were reapplied in the optimization problems for both Scenarios a and b, and the comparison of different cost models is shown in Figure 17. The use of different cost models does not affect the optimal design capacities of the compressor and thermal storage, meaning only the compressor CAPEX changes. In Scenario a, the variation in cost models results in a wide range of compressor CAPEX, from under 200,000 USD to nearly 1000,000 USD, accounting for 30% to almost 70% of the total CAPEX, which significantly impacts the TAC across all cases. For most models that yield a high compressor CAPEX (above 400,000 USD), the TAC for the MVR at a fixed electricity price of 154 €/MWh is lower than that of the FVC. However, the opposite is true when the compressor CAPEX is less than 400,000 USD, as seen in the cases of centrifugal compressors in the Peters' model and reciprocating compressors in the Seider's model. This demonstrates that a lower compressor CAPEX and its smaller share of total CAPEX are favorable for the proposed FVC distillation approach. When the fixed electricity price increases to 180 €/MWh, the FVC shows significant cost advantages in all cost model cases. These results highlight that the choice of cost model influences the optimal design and operation of the FVC distillation system, making it crucial to select the most appropriate cost model, particularly for multistage compressors.

In Scenario b, all models yield consistent results when comparing and ranking the TAC of MVR and FVC. The MVR's TAC at an electricity price of 115 USD/MWh is the lowest, followed by the FVC. Although the compressor CAPEX varies significantly, as in Scenario a, its share of the total CAPEX is higher, reaching a maximum of 83.3%. This high share, driven by the need for a large compressor capacity, is the main reason for the higher TAC of the FVC. Despite this, the conclusion remains that the FVC becomes competitive when the fixed electricity price is double the off-peak price. If compressor CAPEX can be reduced, a 1.5 times difference between fixed and off-peak electricity prices would make the FVC economically advantageous, particularly if the lower compressor cost models from Scenario a are applied. Overall, Scenario b requires greater compressor CAPEX reduction for the FVC to be preferred, whereas Scenario a demonstrates advantages under current compressor cost estimates.

## 6 | CONCLUSIONS

This research introduces a novel approach to designing load-adaptable, electrified distillation processes by integrating FVC with thermal storage. Various configurations of the FVC and thermal storage are analyzed to gain insights into energy efficiency and storage requirements, showing that FVC outperforms MVR in terms of electricity consumption and heat output. Optimization models for systematic design and scheduling are developed to determine the optimal design and scheduling of the FVC and thermal storage under both time-varying and fixed peak/off-peak electricity pricing scenarios. The proposed distillation approach demonstrates flexibility in responding to dynamic electricity markets, offering economic potential,

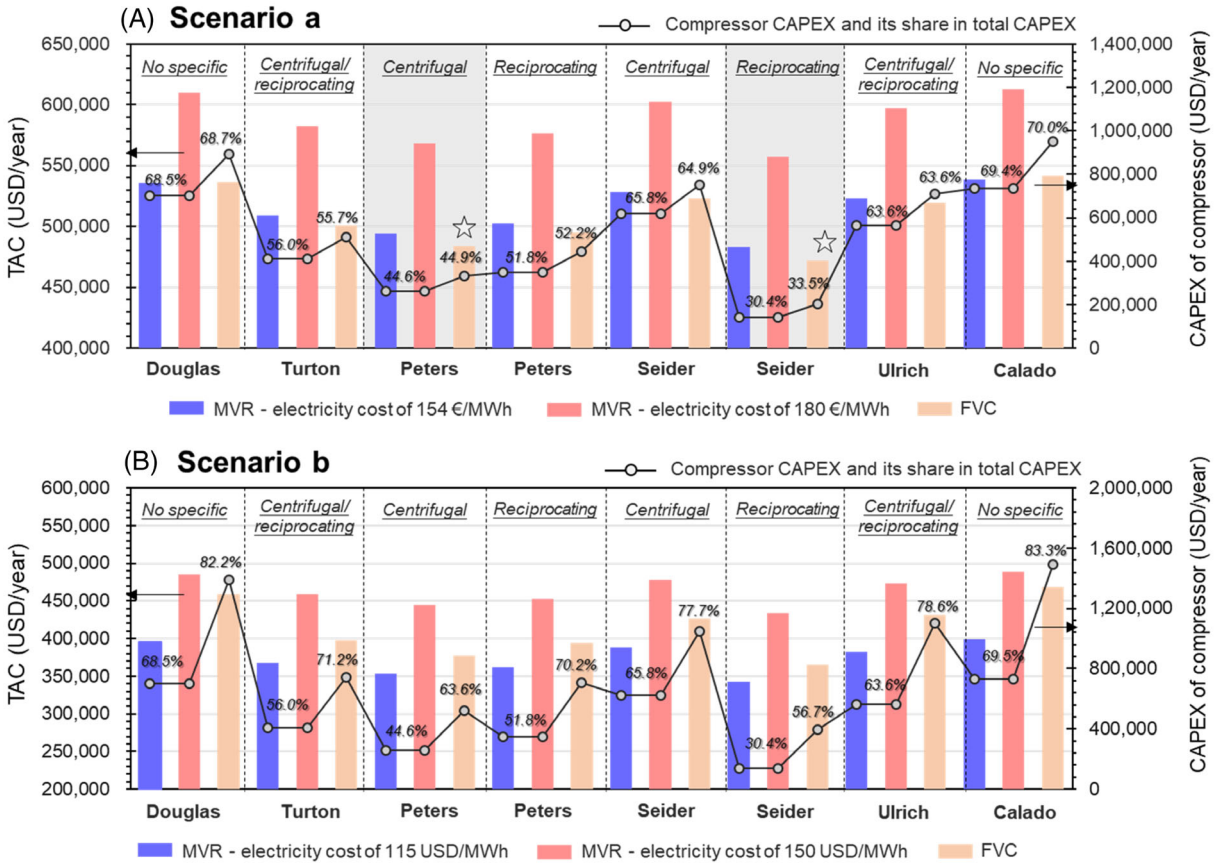


**FIGURE 17** Comparison of TAC and compressor CAPEX using different compressor cost models: (A) results for Scenario a; (B) results for Scenario b.

particularly in reducing OPEX. Greater reduction potential is found with time-varying electricity prices, leading to an OPEX reduction of 6%–24%. These specific reductions may vary depending on different electricity markets.

However, the high CAPEX of compressors remains a challenge, significantly influencing the TAC. A key finding is the importance of selecting appropriate compressor cost models, as different models resulted in substantial CAPEX variation, especially for the FVC. Lower compressor costs favor the FVC's economic viability. In conclusion, FVC combined with thermal storage is preferred over MVR in cases with highly variable electricity prices and low compressor CAPEX. The high CAPEX of the compressor, particularly in multistage configurations, is a key factor limiting the feasibility of FVC. Future research should focus on reducing compressor costs and exploring advanced compressor technologies to improve the economic viability of FVC in load-adaptable distillation processes. Additionally, electricity pricing plays a significant role in determining OPEX, and different electricity market scenarios should be evaluated on a case-by-case basis to fully assess the economic potential of the proposed system.

While the proposed distillation approach shows great potential, there are several limitations in this study that require further investigation. The case study focused solely on water–methanol separation, but additional separation processes, particularly those with high energy demands such as propane-propylene separation, should be explored. Additionally, while the direct storage method is more efficient for heat transfer and reduces the amount of storage medium required in this study, the use of water as a storage medium—drawn directly from the column bottom—may not be applicable for separation tasks that do not involve water purification. Indirect storage methods using different mediums should also be evaluated across various separation tasks. Although this study performed scheduling optimization, the operation of the FVC was assumed to be quasi-stationary. In reality, the system dynamics of the FVC and thermal storage need to be incorporated into the optimization process to account for transient behavior and nonlinear performance changes during scheduling. The use of quasi-stationary models should be further justified by evaluating whether the two critical scheduling units exhibit fast ramp rates and dynamics relative to the 1-h time interval. Moreover, advanced control strategies should be developed for real-time, precise control of column operations in response to fluctuating electricity prices.

At last, this study highlights the importance of flexibility for distillation and introduces a novel approach, but other methods are expected to emerge using different mechanisms and configurations (e.g., distillation design with electric boilers and pressure-varying operations[45]) to design flexible, load-adaptable distillation systems. Developing such approaches would be an essential and exciting step in advancing distillation technologies, revitalizing distillation's role

in response to the evolving energy landscape during the transition to net zero.

## AUTHOR CONTRIBUTIONS

**Meng Qi:** Writing – original draft; conceptualization; methodology; software; formal analysis; validation; investigation; writing – review and editing. **Xiaodong Zhang:** Conceptualization; methodology; validation; writing – original draft; writing – review and editing. **David Shan-Hill Wong:** Conceptualization; methodology; validation; writing – review and editing. **Chi-Min Shu:** Conceptualization; methodology; validation; writing – review and editing. **Chengtian Cui:** Conceptualization; methodology; validation; formal analysis; supervision; writing – original draft; funding acquisition; writing – review and editing. **Anton A. Kiss:** Conceptualization; methodology; validation; writing – original draft; supervision; formal analysis; writing – review and editing.

## ACKNOWLEDGMENTS

This work was supported by the National Natural Science Foundation of China (nos. 22408402, 22208164), the Shandong Postdoctoral Science Foundation (no. SDBX2023020), and the Natural Science Foundation of Jiangsu Province (no. BK20220348).

## CONFLICT OF INTEREST STATEMENT

The authors declare there is no conflict of interest.

## DATA AVAILABILITY STATEMENT

Figures 1–4 and 8–10 are graphical representation of process flowsheet or conceptual designs, so there is no numerical data associated with them. The Aspen Plus simulation procedure for reproducing the numerical data presented in Figures 5–7 is detailed in the "FVC Simulation and Analysis" section of Appendix S1. Additional information on the ALAMO surrogate modeling approach and TAC estimation is also provided in this file. Numerical data supporting Figures 11–17, including electricity price data, optimization results, cost estimations, and thermal storage profiles, can be found in Appendix S2 Excel file. Simulation files and Python/GAMS codes used for optimization are available upon request.

## ORCID

*Meng Qi* https://orcid.org/0000-0002-7323-6773
*Chengtian Cui* https://orcid.org/0000-0002-1270-2275

## REFERENCES

1. Schiffer ZJ, Manthiram K. Electrification and decarbonization of the chemical industry. *Joule*. 2017;1(1):10-14.
2. Mallapragada DS, Dvorkin Y, Modestino MA, et al. Decarbonization of the chemical industry through electrification: barriers and opportunities. *Joule*. 2023;7(1):23-41.
3. Sholl DS, Lively RP. Seven chemical separations to change the world. *Nature*. 2016;532(7600):435-437.
4. Chavez Velasco JA, Tawarmalani M, Agrawal R. Which separation scenarios are advantageous for membranes or distillations? *AIChE J*. 2022;68(11):e17839.
5. Kim J-K. Studies on the conceptual design of energy recovery and utility systems for electrified chemical processes. *Renew Sustain Energy Rev*. 2022;167:112718.
6. Tsouris C, Blankenship KD, Dong J, DePaoli DW. Enhancement of distillation efficiency by application of an electric field. *Ind Eng Chem Res*. 2001;40(17):3843-3847.
7. Cui C, Zhang Q, Zhang X, Sun J, Chien IL. Process synthesis and plant-wide control of intensified extractive distillation with preconcentration for separating the minimum-boiling azeotropes: a case study of acetonitrile dehydration. *Sep Purif Technol*. 2022;285:120397.
8. Cui C, Qi M, Zhang X, et al. Electrification of distillation for decarbonization: an overview and perspective. *Renew Sustain Energy Rev*. 2024;199:114522.
9. Oliveira C, Van Dril T. Decarbonisation options for large volume organic chemicals production, Sabic geleen. *Energy and Climate Change*. PBL Netherlands Environmental Assessment Agency: The Hague; 2021.
10. Jana AK. Advances in heat pump assisted distillation column: a review. *Energy Conversion Manage*. 2014;77:287-297.
11. Kiss AA. *Advanced Distillation Technologies: Design, Control, and Applications*. John Wiley & Sons; 2013.
12. Kiss AA. Distillation technology – still young and full of breakthrough opportunities. *J Chem Technol Biotechnol*. 2014;89(4):479-498.
13. Kiss AA, Flores Landaeta SJ, Infante Ferreira CA. Towards energy efficient distillation technologies – making the right choice. *Energy*. 2012;47(1):531-542.
14. He W, King M, Luo X, Dooner M, Li D, Wang J. Technologies and economics of electric energy storages in power systems: review and perspective. *Adv Appl Energy*. 2021;4:100060.
15. Chen C, Yang A. Power-to-methanol: the role of process flexibility in the integration of variable renewable energy into chemical production. *Energy Conversion Manage*. 2021;228:113673.
16. Qi M, Vo DN, Yu H, et al. Strategies for flexible operation of power-to-X processes coupled with renewables. *Renew Sustain Energy Rev*. 2023;179:113282.
17. Wang R, Ma J, Sheng H, Zavala VM, Jin S. Exploiting different electricity markets via highly rate-mismatched modular electrochemical synthesis. *Nat Energy*. 2024;9(9):1064-1073.
18. Qi M, Lee J, Hong S, et al. Flexible and efficient renewable-power-to-methane concept enabled by liquid $CO_2$ energy storage: optimization with power allocation and storage sizing. *Energy*. 2022;256:124583.
19. Smith C, Torrente-Murciano L. The importance of dynamic operation and renewable energy source on the economic feasibility of green ammonia. *Joule*. 2024;8(1):157-174.
20. Svitnič T, Sundmacher K. Renewable methanol production: optimization-based design, scheduling and waste-heat utilization with the FluxMax approach. *Appl Energy*. 2022;326:120017.
21. Kister HZ. *Distillation Design*. Vol 1. McGraw-Hill; 1992.
22. El Wajeh M, Mhamdi A, Mitsos A. Optimal design and flexible operation of a fully electrified biodiesel production process. *Ind Eng Chem Res*. 2024;63(3):1487-1500.
23. Isogai H, Nakagaki T. Power-to-heat amine-based post-combustion $CO_2$ capture system with solvent storage utilizing fluctuating electricity prices. *Appl Energy*. 2024;368:123519.
24. Seo K, Retnanto AP, Martorell JL, Edgar TF, Stadtherr MA, Baldea M. Simultaneous design and operational optimization for flexible carbon capture process using ionic liquids. *Comput Chem Eng*. 2023;178:108344.
25. Zhang Q, Grossmann IE, Heuberger CF, Sundaramoorthy A, Pinto JM. Air separation with cryogenic energy storage: optimal scheduling considering electric energy and reserve markets. *AIChE J*. 2015;61(5):1547-1558.
26. Tsay C, Kumar A, Flores-Cerrillo J, Baldea M. Optimal demand response scheduling of an industrial air separation unit using data-driven dynamic models. *Comput Chem Eng*. 2019;126:22-34.
27. Caspari A, Offermanns C, Schäfer P, Mhamdi A, Mitsos A. A flexible air separation process: 1. Design and steady-state optimizations. *AIChE J*. 2019;65(11):e16705.

28. Caspari A, Offermanns C, Schäfer P, Mhamdi A, Mitsos A. A flexible air separation process: 2. optimal operation using economic model predictive control. *AIChE J*. 2019;65(11):e16721.
29. Yang D, Zhang Q, Zhang Q, Cui C. Dynamics and control of electrified pressure-swing distillation for separating a maximum-boiling azeotrope featuring small pressure-induced shift. *Sep Purif Technol*. 2023;312:123360.
30. Cui C, Zhang Q, Zhang X, Sun J, Chien I-L. Dynamics and control of thermal-versus electrical-driven pressure-swing distillation to separate a minimum-boiling azeotrope. *Sep Purif Technol*. 2022;280:119839.
31. Cui C, Zhang X, Qi M, Lyu H, Sun J, Kiss AA. Fully electrified heat pump assisted distillation process by flash vapour circulation. *Chem Eng Res Des*. 2024;206:280-284.
32. Dumont O, Frate GF, Pillai A, Lecompte S, Lemort V. Carnot battery technology: a state-of-the-art review. *J Energy Storage*. 2020;32:101756.
33. Shen Z, Qu Q, Chen M, Lyu H, Sun J. Advancements in methanol distillation system: a comprehensive overview. *Chem Eng Res Des*. 2023;199:130-151.
34. Mucci S, Mitsos A, Bongartz D. Cost-optimal power-to-methanol: flexible operation or intermediate storage? *J Energy Storage*. 2023;72:108614.
35. Allman A, Palys MJ, Daoutidis P. Scheduling-informed optimal design of systems with time-varying operation: a wind-powered ammonia case study. *AIChE J*. 2019;65(7):e16434.
36. Cozad A, Sahinidis NV, Miller DC. Learning surrogate models for simulation-based optimization. *AIChE J*. 2014;60(6):2211-2227.
37. ENTSO-E Transparency Platform. ENTSO-E: day ahead prices and power generation data. https://transparency.entsoe.eu/
38. Qi M, Cui C, Yu H, He T, Zhao D. Synergies between Carnot battery and power-to-methanol for hybrid energy storage and multi-energy generation. *J Clean Prod*. 2023;430:139548.
39. Luyben WL. Capital cost of compressors for conceptual design. *Chem Eng Process Process Intensification*. 2018;126:206-209.
40. Douglas JM. *Conceptual Design of Chemical Processes*. McGraw-Hill Professional; 1988.
41. Turton R, Bailie RC, Whiting WB, Shaeiwitz JA. *Analysis, Synthesis and Design of Chemical Processes*. Pearson Education; 2008.
42. Peters MS, Timmerhaus KD. *Plant Design and Economics for Chemical Engineers*. McGraw-Hill International; 1990.
43. Seider WD, Lewin DR, Seader J, Widagdo S, Gani R, Ng KM. *Product and Process Design Principles: Synthesis, Analysis, and Evaluation*. John Wiley & Sons; 2017.
44. Ulrich GD. *A Guide to Chemical Engineering Process Design and Economics*. Wiley; 1984.
45. Udugama IA, Taube MA, Kirkpatrick R, Bayer C, Young BR. Implications for control systems in highly volatile energy markets: using a high purity distillation electrification case study. *Chem Eng Res Des*. 2024;203:431-440.


## SUPPORTING INFORMATION

Additional supporting information can be found online in the Supporting Information section at the end of this article.

**How to cite this article:** Qi M, Zhang X, Wong DS-H, Shu C-M, Cui C, Kiss AA. Electrified distillation with flash vapor circulation and thermal storage for dynamic electricity markets. *AIChE J*. 2025;71(5):e18750. doi:10.1002/aic.18750